JOURNAL OF PROPULSION AND POWER
Vol. 17, No. 6, November–December 2001

Synthesis of a FESTIP Airbreathing TSTO Space Transportation System

H. Grallert*
Astrium Space Infrastructure, 81663 Munich, Germany

The recent Future European Space Transportation Investigation Program (FESTIP) system study has included one two-stage-to-orbit (TSTO) concept with an airbreathing first stage and a rocket-propelled second stage. Because of the pure acceleration mission from Kourou/CSG and the limited technology level that should be applied, turbojet engines for staging at Mach 4 were assumed in the first stage. Two different TSTO configurations were studied in parallel: the fully integrated delta-wing configuration and the less integrated trapezoidal-wing configuration. The predesign activities were completed in July 1998, and a better data basis is now available for comparing the two design options in terms of launcher size, performance, complexity, operations, and cost. In spite of the high aerodynamic integration of the delta-wing configuration, its overall performance is rather limited because of weak turbojet performance at high Mach numbers and altitudes. Inclusion of a ramjet for operation beyond Mach 3 would increase the optimum staging Mach number and overall complexity of this TSTO concept. The trapezoidal-wing configuration makes best use of a boost to beyond Mach 1.3 by rocket engines of the second stage, which are fueled during the combined ascent by cross feeding from the first stage. The limited analyses performed on the double-wing aerodynamic interaction between the mated stages has not revealed any severe objections. This TSTO concept has exceeded the current FESTIP performance requirements, delivering 9 Mg into equatorial 250-km-reference orbit and 3 Mg into polar 250-km-reference orbit. With respect to cost, this launcher could be optimized by avoiding any stage integration. Then the internal tank arrangement of the first stage is not penalized by additional geometric constraints, and stage separation becomes simpler. Takeoff mass of the trapezoidal-wing configuration is 470 Mg compared to 430 Mg for the delta-wing configuration. Nevertheless, the vehicle dry mass, which drives development cost, is 40 Mg heavier for the delta-wing configuration. The absolute cost figures of both TSTO options are significantly higher than those of the single-stage-to-orbit vehicles investigated in the FESTIP program.

Introduction

FROM 1994 to 1998, the Future European Space Transportation Investigation Program (FESTIP)[1] has been performed by a combined European team under ESA contract. One basic element of this program was the FESTIP system study, which was performed by an European engineering team colocated in Munich/Ottobrunn and led by Astrium (former DaimlerChrysler Aerospace). A variety of different advanced space transportation concepts was investigated with the same set of mission requirements and engineering assumptions. The FESTIP two-stage-to-orbit (TSTO) concept FSSC-12 takes off and lands horizontally with airbreathing propulsion in the first stage and rocket propulsion in the second stage (orbiter). It was initially derived from the SÄNGER concept,[2] taking into account the different FESTIP mission and system requirements. The major challenge was the implementation of an adequate first-stage configuration. Because the SÄNGER configuration and its propulsion concept was not the best solution for redesign to the FESTIP mission and system requirements, a new configuration was investigated. Two different configurations were studied in parallel: the fully integrated configuration with very well mated stages and blended interface area, and the less integrated configuration with belly-to-back stage mating without blending of the interface area. For both options the orbiter design was kept constant.

The takeoff from Kourou Centre Spatiale Guiane (CSG) does not require a cruise-out phase. The pure acceleration ascent then drives the first-stage design for maximum thrust minus drag, thus leading to a wing-on-fuselage design instead of a blended-body design. The optimum stage separation Mach number was found at Mach 4 by means of the down-selection process of airbreathing propulsion systems in an earlier study phase of the FESTIP system study.[1] A pure turbojet propulsion system was selected for the first stage because this propulsion concept is most attractive with respect to near-term availability of enabling technology, accuracy of performance prediction, launcher complexity, and development risk. All the other airbreathing propulsion system concepts would increase system complexity and cost. For example, the implementation of a ramjet for Mach 3+ operation would shift the optimum staging beyond Mach 5, thus increasing the thermomechanical loads onto the first stage structure.

Design Rationale

All of the airbreathing vehicles have to be optimized with respect to a high thrust-minus-drag acceleration for passing through the transonic regime. This is caused by the typical thrust characteristics of airbreathing engines (at least of turbojet engines), which always decrease with increasing altitude and flight Mach numbers. Thrust minus drag can alternatively be increased by additionally installed thrust, and/or by decreasing the total drag of the combined configuration. These possible alternatives are leading to very different first-stage designs that can be categorized as two extreme solutions.

The less integrated option was expected to lead to the most cost effective TSTO configuration. The fully integrated option could make use of the existing comprehensive database of SÄNGER.[2] To keep the propulsion system mass as low as possible, the installed total thrust of the airbreathing engines was selected for the average thrust demand for properly accelerating the combined configurations until stage separation. The peak demand in total thrust had to be provided by different means as described next.

Second-Stage Configuration

The aerodynamic shape and design of the orbiter (Fig. 1) were adopted from the initial HORUS configuration[3] used for SÄNGER. For this study the orbiter size had to be increased according to

Received 4 June 2000; revision received 30 October 2000; accepted for publication 29 December 2000.

*Senior System Engineer, Development of Propulsion Stages and Transportation Systems.

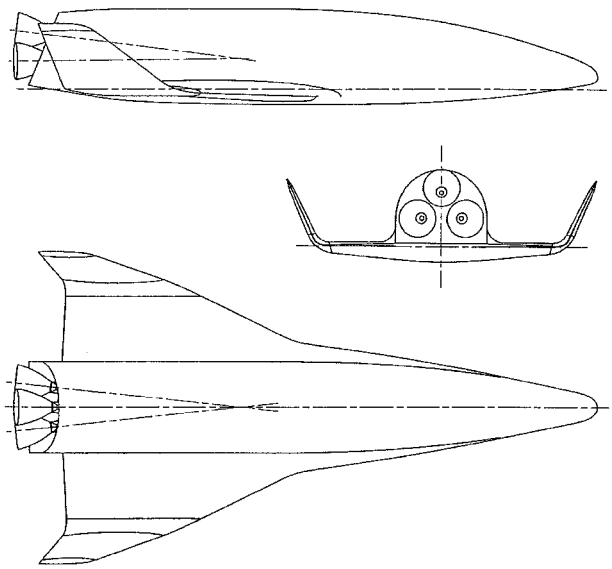

Fig. 1 Aerodynamic configuration of the orbiter.

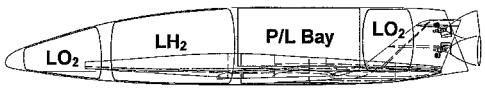

Fig. 2 Inboard arrangement of the orbiter.

the propellant requirements of the FESTIP polar reference mission that defines the maximum tank volumes. The vehicle has a total fuselage length of 38.0 m and a wing span of 20.7 m. The in-board arrangement of the orbiter is shown in Fig. 2. It is different from the original HORUS design. In particular the tank arrangement was selected such that the c.g. position is shifted as much forward as possible. The forward propellant tanks [for liquid oxygen (LO_2) and liquid hydrogen (LH_2)] are conformal tanks, whereas the rear LO_2 tank is cylindrical and nonintegral. The nose gear is housed in the space between the two forward tanks. The main undercarriage is accommodated before the wing carry-through structure.

The aerodynamic data were adopted from earlier HORUS studies[3] that have been performed in the scope of SÄNGER and in the Winged Launcher Configurations Study (performed under ESA contract). The actual aerodynamic reference area has increased to 366.1 m^2.

For safety reasons (engine-out capability, abort maneuvers) three main engines were selected at a thrust level of 800 kN each. The three main engines and the two engines of the orbital maneuvering system (OMS) are accommodated in the engine bay compartment. The engine integration with two main engines at the lower base area and one main engine at the upper base area allows engine turn (gimbal) by ±6 deg. A staged combustion cycle engine was used with 244.5 bar thrust chamber pressure, 7.2 oxidizer-to-fuel mixture ratio, and a nozzle expansion ratio of 275. The vacuum specific impulse is 465.4 s. and the thrust-to-weight ratio in vacuum is 59.5. For the OMS two HM7-derived engines are proposed at a thrust level of 75 kN each. Their position is at the vehicle base area, left and right of the upper main engine. The reaction control system (RCS) is composed of 16 gaseous hydrogen and oxygen thrusters with a thrust level of around 400 N each. This thruster size was selected because no rendezvous and docking maneuvers have to be performed (FESTIP requirements). The support of the aerodynamic control means during reentry and descent will ask also for larger RCS thrusters as can be seen in the space shuttle design; however, this was not considered in detail. The propulsion system architecture is based on a unified system for the main engines and OMS engines, and on decentralized clusters of RCS thrusters.

All of the orbiter ascent calculations were performed by means of trajectory optimization software [advanced launchor trajectory optimization software (ALTOS[4])] together with the ascent of the combined configuration. For the polar mission orbiter lift-off mass is 193 Mg, and the ascent propellant mass is 154.5 Mg. These were held constant, whereas the stage separation conditions vary depending on the related first-stage design option.

Table 1 Summary of the orbiter mass budgets

Items	Budgets (Mg)
Fuselage structure	6.47
Wings and winglets	3.16
Propellant tanks and cryoinsulation	4.61
Secondary structure	0.59
TPS	6.15
Main engines	4.61
OMS engines	0.35
Landing gear	1.25
Actuation/hydraulics	0.59
Electric system, SPS and harness	1.89
Propellant supply system	1.37
RCS	0.03
Cross feeding system	0.17
Avionics	0.15
Vehicle dry mass	31.39
Residuals and propellant margins	1.68
OMS/RCS propellants	2.37
Usable main propellants	154.50
Payload mass into polar orbit	2.99
Lift-off mass	192.93

The thermally protected structure is based on a fuselage from carbon fiber reinforced plastic and frames from aluminum alloys. The thermal protection system (TPS) is composed of a flexible external insulation, metallic multiwall TPS, and shingles from carbon silicon carbide. Only the nose cap and the rudders are hot elements. Reentry calculations with ALTOS have shown that the FESTIP cross-range requirements are met at a heat load level of 350 kW/m^2 at the stagnation point.

The orbiter mass breakdown for the polar mission is shown in Table 1. It contains 14% mass margins on structural components, 12% on the propulsion system, and 10% on subsystems. The vehicle dry mass is 31.4 Mg including the cross-feeding system for the less integrated TSTO. It is 150 kg less for the orbiter of the fully integrated TSTO option where no cross-feeding system has to be integrated.

First-Stage Design and Performance

General Considerations

Two different concepts were considered for implementing the new first-stage configuration. One is characterized by installing additional thrust for overcoming the higher drag of the less refined aerodynamic configuration. The orbiter must not be well integrated in the back of the first stage, leading to a less integrated configuration. The wing shape is independent from the orbiter wing and a trapezoidal wing type with hypersonic leading edge was chosen. This vehicle option is called Trapezoidal Wing Concept (FSSC-12T). There are different options for increasing the actual engine thrust. The best solution found is the use of the orbiter rocket engines instead of increasing the thrust level of the airbreathing engines. This leads to the requirement to cross feed the orbiter engines from additional tanks that have to be installed in the first stage. During the cross-feeding operation, the orbiter base area is widely filled by the recirculating gas of the rocket plumes and thus reduces its contribution to vehicle drag.

The second concept is characterized by optimizing the aerodynamic configuration for providing minimum vehicle drag. This can be achieved with a slender body configuration with low wave drag of the wing and minimum stage integration drag. The latter leads to the requirement to highly integrate the orbiter into the back of the first stage. Because the body widths of both stages are of equal size, this integration includes also the orbiter wings, whereas the large orbiter base area is still affecting drag. For closely integrating the two wings, a large delta wing is required for the first stage. Therefore, this vehicle option is called Delta Wing Concept (FSSC-12D). The cross-sectional profile must show a steady and smooth curve without steep gradients.

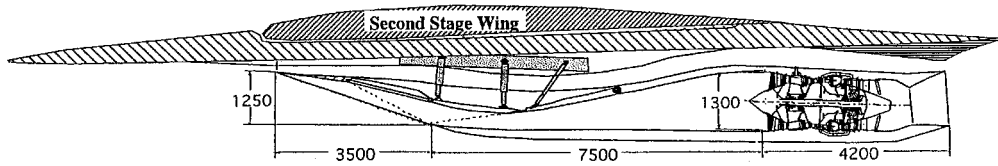

Configuration for Delta Wing Concept with Precompression and Diverter Duct (similar final Nacelle Configuration for Trapezoidal Wing Concept)

Fig. 3 Turbojet engine integration below the wings.

It was not evident which of the two alternatives for optimizing thrust minus drag is the better choice with respect to complexity and cost. Therefore, both solutions were investigated in parallel in the two design loops.

The required total thrust level of the turbojet engines of ~3150 kN was divided into eight units, consistent with the maximum engine size that can be tested at existing European engine test facilities. Eight 394-kN thrust engines integrated in the fuselage bottom require a maximum fuselage width of 10 m at least. Because these airbreathing engines cannot be accommodated in a nonlenticular fuselage (cylindrical cross section), the engines had to be clustered in nacelles below the wings. Different airbreathing engine arrangements were evaluated. As a compromise between flow symmetry and different precompression length in front of the air intakes, boundary-layer effects, and clearance from ground during takeoff and landing, the nacelle type with four parallel turbojet engines was selected. The turbojet engines require a boundary-layer diverter between the lip of the first air-intake ramp and the underside of the wing.

The main characteristics of the turbojet engines are summarized in Ref. 5. All aerodynamic losses of the engine/nacelle installation were included in the installed engine performance data. For simulating fly-back performance, additional turbojet engine performance data were implemented on a 10-kPa return trajectory at part dry power setting. The scheme of turbojet engine integration below the first stage wings is shown in Fig. 3.

Whereas a complete aerodynamic dataset was available for the orbiter from earlier system studies,[3] the aerodata of the new combined TSTO configuration had to be implemented in this study. Normally this is a comprehensive and time-consuming procedure. The aerodynamic data were implemented by 1) handbook and panel methods; 2) comparison with existing airplane data (SR-71, B-70, SÄNGER, Boeing-BETA II, DLR-DSL); and 3) common buildup of the data for trapezoidal- and delta-wing configuration.

The remaining uncertainty with the aerodynamic data has mainly originated in the 1) unknown interaction effects between the wings of the first and second stage of the trapezoidal-wing configuration (biplane effect); 2) unknown near-field effects during stage separation, in particular for the delta-wing configuration (suction forces and moments); and 3) unknown aerodynamic lee-side effects during fly-back of the delta-wing configuration (caving of wing and fuselage upper side).

Despite the lower staging Mach number (Mach 4), stage separation is still a demanding procedure because 1) launch mass ratio of the stages is below one (0.75 for the trapezoidal-wing configuration and 0.93 for the delta-wing configuration); 2) specific flight maneuvers of the combined configuration (zero-g maneuver, engine throttle) are required for providing favorable conditions prior to staging; and 3) near-field aerodynamic effects are encountered during physical separation of the two stages, thus disturbing the balance of forces and moments that was achieved with the combined configuration.

In general, the following initial staging requirements have to be met by the combined configuration for safe separation: 1) flight maneuver for providing a very low z-force level ($n_z \approx 0$) and low angle-of-attack ($\alpha \leq 2$ deg); 2) thrust balancing between the orbiter and the first stage for providing a low x-force level (maximum difference allowed is 200 kN); and 3) sufficient trim and control capability in both stages during staging.

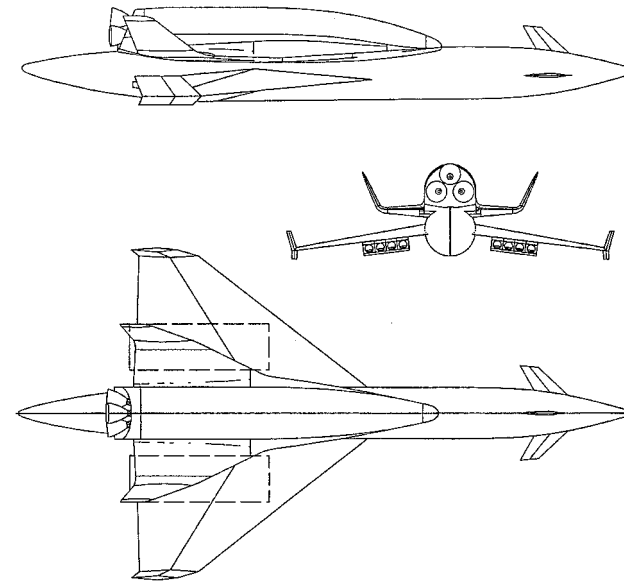

Fig. 4 Plan view of the latest trapezoidal-wing configuration: length 72 m, wing span 36.6 m.

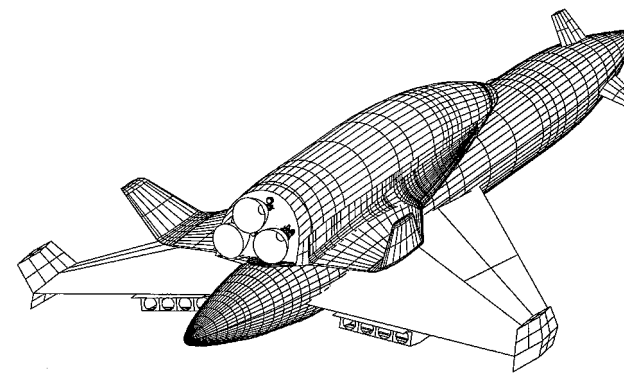

Fig. 5 CAD drawing of the latest trapezoidal-wing configuration.

Trapezoidal-Wing Configuration

The latest trapezoidal-wing configuration achieved in FESTIP is shown in Figs. 4 and 5. Mass data for the equatorial orbit mission are summarized in Table 2. The major design features of this TSTO option are 1) trapezoidal wing-on-fuselage configuration; 2) middle decker with unhedral wing (the wings of the two stages are producing a biplane effect); 3) increased sweep angle of the leading edge for improving engine/airframe integration (precompression in front of the air intake, lift providing wing section); 4) slender fuselage with circular cross section, length (72 m) adapted to the volumetric propellant requirements; 5) engines clustered in two nacelles, which are mounted below the wings; 6) wing tip mounted stabilizers; 7) nose fin for increasing lateral stability; and 8) all-movable foreplanes for increasing pitch control.

Table 2 Mass budget summary for the first stages

Items	FSSC-12T (Mg)	FSSC-12D (Mg)
Fuselage structure	40.57	48.40
Wings and stabilizers	27.44	50.95
LH_2 tanks and cryoinsulation	4.57	5.02
LOX tank and cryoinsulation	1.64	0.00
Stage separation system	1.10	8.82
Main engines	42.00	44.10
Landing gear	15.61	14.19
Actuation/hydraulics	3.16	3.85
Electric system, SPS and harness	4.69	5.72
Propellant supply system	6.16	6.44
Avionics	1.00	1.00
Vehicle dry mass	147.95	188.49
Residuals and margins	1.33	0.42
Ascent propellants (LH_2 or $LH_2 + LO_2$)	119.20	36.40
Fly-back/landing propellant (LH_2)	4.80	7.00
Propellant reserve (LH_2)	0.50	0.70
Second stage mass	199.36	197.12
Total launch mass	473.14	430.13

The thrust increase needed for the trapezoidal-wing concept is bound to the parallel operation of airbreathing engines of the first stage and the rocket engines of the orbiter from Mach 1.3 up to stage separation (Mach 4). To avoid an increased orbiter dry mass, the additional tanks for this early rocket operation are installed in the first stage. This requires a propellant cross-feeding system, i.e., propellant feeding from the first stage to the orbiter. It was assumed that the required equipment is very similar to the cross-feeding system of the space shuttle.[6] Optionally, also a small buffer system can be used in the orbiter. The buffer system allows disconnecting the feeding lines at stage separation while the engines are still running. In essence, the rocket engines are being throttled down for 4 s to provide low excess thrust at stage separation. At this mission event the feeding lines are supposed to be separated from first stage tank supply to orbiter tank supply. Once the disconnector valves are operated, the separated cross-feeding pipes in the orbiter must be vented. The residual propellants in these pipe segments are rather small (total mass 129 kg) because the pipe diameter will not exceed 0.25 m and the tube length is limited to 2 m each. The equipment masses were assessed by means of the masses quoted for the respective space shuttle parts: 150 kg were accounted for the Orbiter and 900 kg for the first stage.

Thrust balance during stage separation was achieved for the trapezoidal-wing configuration by throttling the orbiter engines to around 30%. This can be realized by a short decrease in the oxidizer-to-fuel mixture ratio (throttling of the LO_2 supply), which has already been demonstrated with the Russian RD-0120 in the RECORD project.[7] This leads to 685-kN total rocket thrust compared to 512-kN total airbreathing thrust at stage separation. For the trapezoidal-wing configuration a solid rocket motor separation system is proposed. The five separation motors (two forward, three aft with 125 kN thrust each) push down the first stage with around 0.4 g_o normal acceleration. The total mass of the required stage separation equipment was assessed below 1 Mg. The airframe structure has to be locally enforced at the three stage-interface points.

The stage separation procedure is illustrated by the sequence shown in Fig. 6. The whole procedure lasts 8 s, with just 3 s required at the orbiter rocket engine throttling condition. The zero-lift flight maneuver is included in the nominal ALTOS ascent trajectory of the combined configuration. The separation window is rather limited with respect to aerodynamic dispersions. Aerodynamic near-field interaction effects were not considered.

Delta-Wing Configuration

The latest delta-wing configuration achieved in FESTIP is shown in Figs. 7 and 8. Mass data for the equatorial orbit mission are summarized in Table 2. The major design features of this TSTO option are 1) double delta-wing-on-fuselage configuration; 2) shoulder decker for allowing a perfect wing/wing integration between the two stages, caving of the vehicle back for better orbiter integration; 3) slender fuselage with circular cross section adapted to volumetric requirements (final fuselage length 86 m); 4) two large stabilizers that are in line with and aft of the orbiter winglets; 5) engines clustered in two nacelles, which are mounted in a rearward position below the wings; and 6) all-movable foreplanes for increasing pitch control.

The proper wing/wing integration has produced a slightly negative zero-lift wing angle (−2 deg). Details of this integration are shown in Fig. 9.

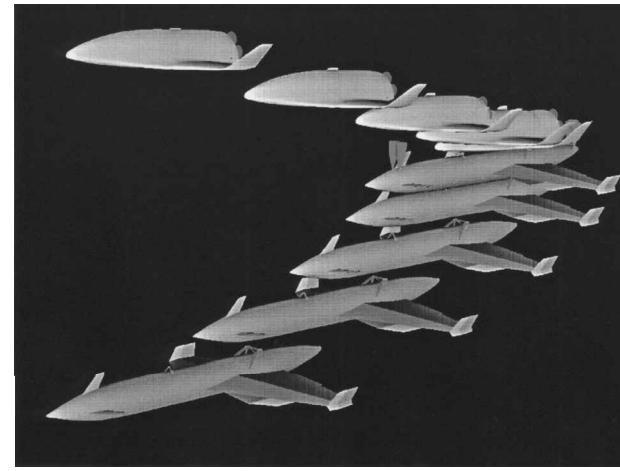

Fig. 6 Stage separation sequence of the trapezoidal-wing configuration.

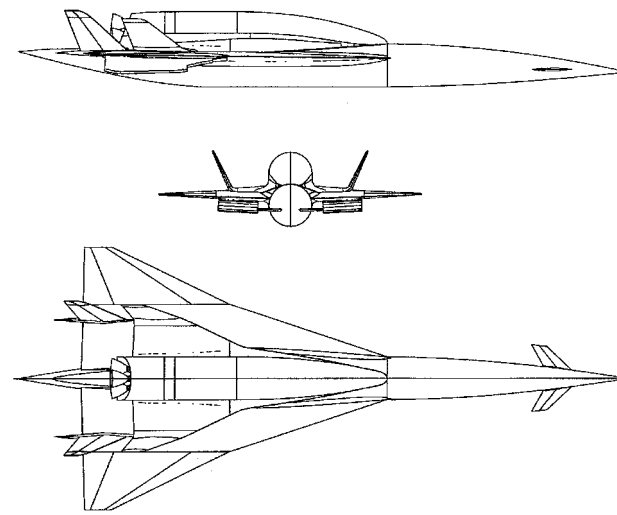

Fig. 7 Plan view of the latest delta-wing configuration: length 86 m, wing span 37 m.

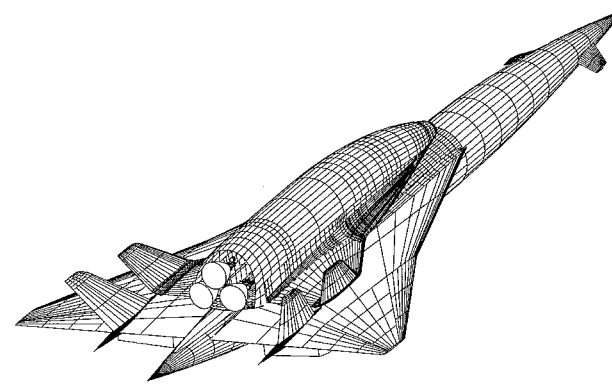

Fig. 8 CAD drawing of the latest delta-wing configuration.

Table 3 Comparison of alternative FSSC-12 first-stage configurations

Criterion/issue	Trapezoidal-wing configuration	Delta-wing configuration
Vehicle size	72 m in length	86 m in length
Vehicle mass (hot structure)	T/O 470 Mg; dry 148 Mg	T/O 430 Mg; dry 188 Mg
Wings	Triangular wing profiles	Caved delta-wing profiles
Fuselage	Cylindrical; 6 m diam	Cylindrical; 6 m diam
Engine/airfr. integration	Precompression effect	Precompression effect
Turbojet engines	100% nominal thrust level	105% nominal thrust level
Stage integration	Only fuselage or none	Fully integrated, footprint
Lateral control means	One nose fin, wing-tip mounted stabilizers	Two large fins behind winglets of the orbiter
Propellant volume	LH_2 and LO_2 tanks; 644 m^3	Only LH_2 tanks; 592 m^3
Ascent performance	9 Mg into 5 deg/250 km, 3 Mg into 98 deg/250 km; weakest performance in the transonic regime	7 Mg into 5 deg/250 km, 1.2 into 98 deg/250 km; weakest performance prior to stage separation
Fly-back performance	3.8 Mg for 350 km distance	~5.6 Mg for 500 km distance
Cross feeding	Two lines with disconnectors; venting during separation	N.A.
Stage separation	Solid rocket motor separation system	Lifting frame + solid rocket motor separation system
Open issues/uncertain areas	Aerodynamic wing interaction during combined ascent	Stage separation aerodynamics
Development cost level (first stage)	~10 BEuro	~12 BEuro

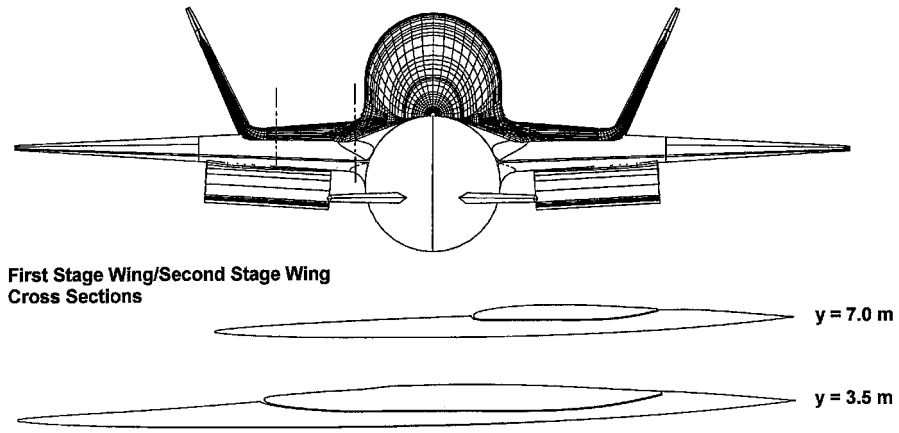

Fig. 9 Wing-to-wing intergration of the delta-wing configuration.

In spite of the high aerodynamic quality of the delta-wing configuration, nominal thrust (8 × 394 kN) was not sufficient for meeting FESTIP performance requirements. Therefore, the installed turbojet engine thrust and size had to be increased by 5%. This has resulted in slightly larger engine nacelle dimensions and mass. Apart from this modification the engine/airframe integration for the delta-wing option is very similar to the latest trapezoidal-wing configuration (see Fig. 3). Because of the large delta-wing area, the nacelles were easily accommodated below the wings. In principle, the diverted boundary layer of the air intakes can be used for a limited filling of the dead area behind the orbiter base area for reducing its drag contribution to the overall drag of the delta-wing configuration.

Beyond Mach 3.5 fuel-rich combustion at an equivalence ratio (EQR) of up to 2.5 was allowed for performing the final pull-up maneuver. Thrust forces of the delta-wing concept were balanced during the staging procedure (main rocket engines ignited and running in idle mode, i.e., at ~30%) by the ignition of the two OMS engines (75 kN each) and by throttling of the turbojet engines from 1300 kN (EQR = 2.5) down to around 800-kN total thrust (EQR = 1). Because of the deep embedding of the orbiter in the caved back of the first stage, a combined lifting-frame/separation motor system is proposed. The solid rocket motor separation system is similar to the one proposed for the trapezoidal-wing configuration. In addition, a lifting frame system is required for providing the necessary clearance of the orbiter and first-stage aeroshells prior to their physical separation. The lifting-frame system has to be designed for the three stage-interface points.

Each of these interface points comprises a frame structure that is linked to both stages with hinges and that is actuated by two hydraulically damped pyro-actuators. The total mass of the combined separation system was determined to be around 7.7 Mg.

Comparison of the Two TSTO Design Options

When comparing the two first-stage design options, the five following areas must be considered (see also Table 3): 1) vehicle size and geometry constraints, 2) vehicle aerodynamics, 3) vehicle overall performance, 4) vehicle structural complexity, and 5) vehicle development cost.

Whereas the wing span and the diameter of the circular fuselage are nearly identical for both configurations (~37 and 6 m, respectively), their fuselage length is very different. For the trapezoidal-wing configuration the length was selected with respect to the accommodation of the tank volumes, which are required for turbojet engine operation plus cross feeding of the orbiter rocket engines. Finally it has approached 72 m. For the delta-wing configuration a body length of 86 m was selected with respect to a high vehicle aspect ratio for providing low wave drag. Notably, despite this length the fuselage volume (1339.5 m^3) and the surface area (1022.5 m^2) are less than those of the trapezoidal-wing configuration (1390.6 m^3 and 1083.2 m^2, respectively). This characterizes the slender body design of the delta-wing configuration.

The major geometry constraint of the delta-wing configuration is defined by the perfect embedding of the orbiter wing into the wing of the first stage. The aerodynamic advantage of a low base drag of the combined configuration has to be weighed against the inherent structural disadvantages of this concept. The perfect stage integration limits any geometric optimization, e.g., the desired shift of the orbiter in axial direction for improving c.g. travels and moments balancing. Also the delta wing is constrained by the minimum projection area that is required for the orbiter wing integration and the profile thickness of the caved wing, which can be accepted from the structural point of view. All these limiting criteria do not apply for the trapezoidal-wing option. With its present configuration

the orbiter is slightly embedded only in the fuselage center, still allowing a longitudinal or/and vertical shift of the orbiter relative to the first stage. That means that the trapezoidal-wing concept offers more flexibility for a future design adaptation and optimization with respect to the present and also new system requirements.

Lift-to-drag ratios vs Mach numbers used in the ALTOS performance calculations are compared in Fig. 10. It is obvious that the aerodynamic quality of the delta-wing configuration is superior in the entire flight regime. The major reason for this difference is the around 40% lower wave drag than for the trapezoidal-wing configuration. Two specific aerodynamic effects are also included in these curves: the interference losses of the two wings of the trapezoidal-wing configuration and the full base drag increment of the orbiter for the delta-wing configuration (beyond Mach 1.3 there are only 25% included for the trapezoidal-wing configuration because the dead area is filled with gas from the rocket plumes). Because of other flight-mechanical constraints (e.g., incidence angle and flight dynamic pressure limitations), at both configurations the maximum possible lift-to-drag ratio could not always be used along the respective ascent trajectory.

The volumetric filling problem of the first stage fuselage arises because of several reasons. The cryogenic propellant tanks are to be integrated only in the fuselage because of the large space required for the LH_2 tanks and the hot structure concept applied. The slender body leads to long cylindrical and/or conical tanks with less structural efficiency. The filling factor of the fuselage is limited because dedicated compartments are housing structural assemblies: wing carry-through structure, support structure at the rear and forward interface points between the stages, undercarriage (Fig. 11).

In this context it must be stressed that the integration of the orbiter into the back of the first stage additionally creates severe tank shaping and tank accommodation problems. The nonintegration of the orbiter would ease significantly the internal arrangement of the center fuselage. The present trapezoidal-wing configuration uses a limited stage integration level. The next design loop would result in a configuration with belly-to-back stage mating as shown in Fig. 12. The delta-wing configuration is limited by the volumetric problems just discused because its overall performance is rather weak and the volume-driving propellant demand is as high as for the less integrated option (44.1 Mg LH_2 compared to 43.5 Mg LH_2).

The latest combined ascent trajectories of both TSTO configurations are compared in Figs. 13–15. For the trapezoidal-wing configuration the following promising solution was found: cross feeding starts at Mach 1.3 and 9 km altitude with 80% rocket engine thrust in parallel to the thrust of the first-stage turbojet engines. This point is met after 199 s from take-off by introducing a short climb segment at constant speed and decreasing flight dynamic pressure. The typical decrease of turbojet thrust at higher Mach/altitude combinations is fully outweighed by increasing rocket thrust. Nominal thrust levels of 100% are sufficient for the turbojet engines. Time to stage separation is 403 s, and the distance from Kourou is 227 km. The stage separation conditions are Mach 4.0, 30 km altitude, 11.9-deg flight-path angle.

For the delta-wing configuration the following compromise was found: ascent along the 50 kPa line. A turbojet engine performance

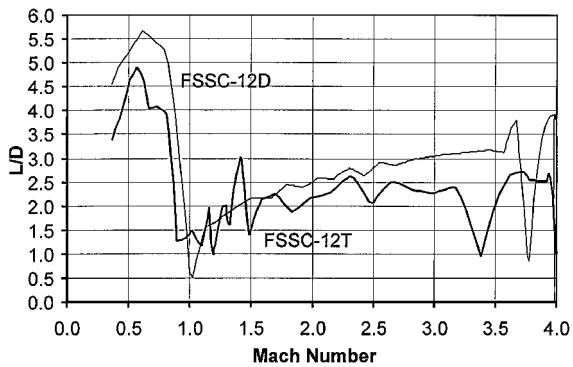

Fig. 10 Comparison of lift-to-drag ratios vs Mach along the respective ascent trajectories.

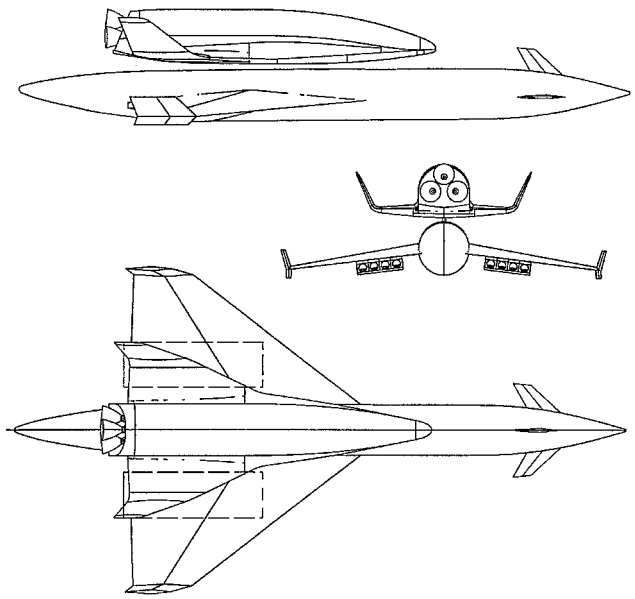

Fig. 12 Trapezoidal-wing configuration with nonintegrated stages.

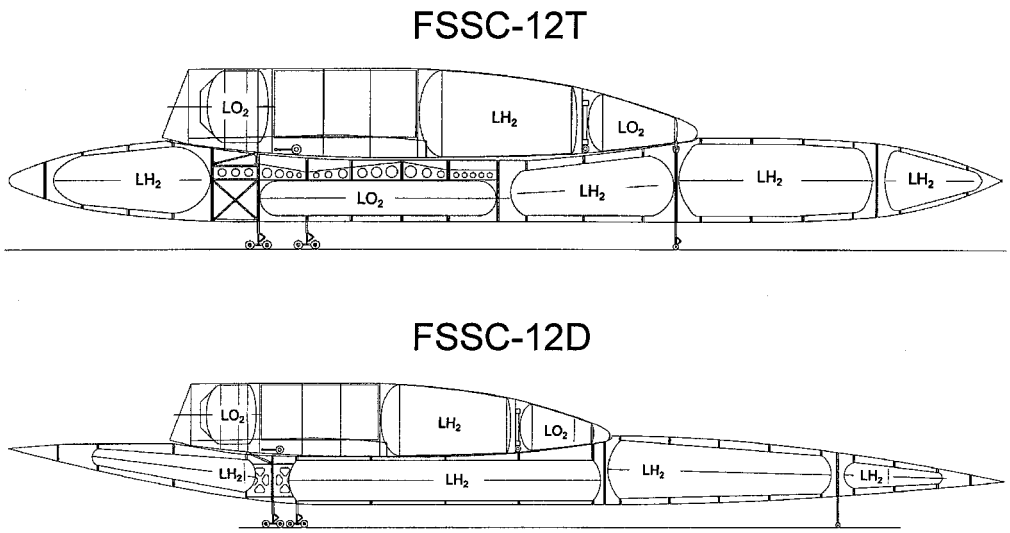

Fig. 11 Inboard arrangement of the two FSSC-12 options.

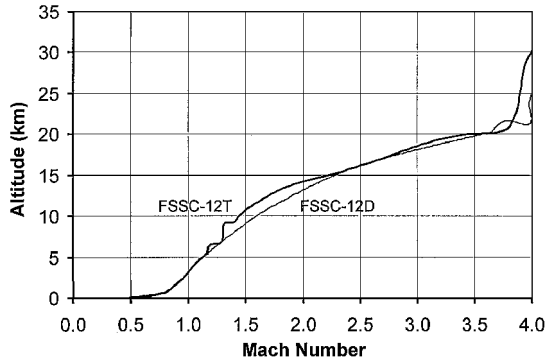

Fig. 13 Comparison of FSSC-12 ascent trajectories up to stage separation.

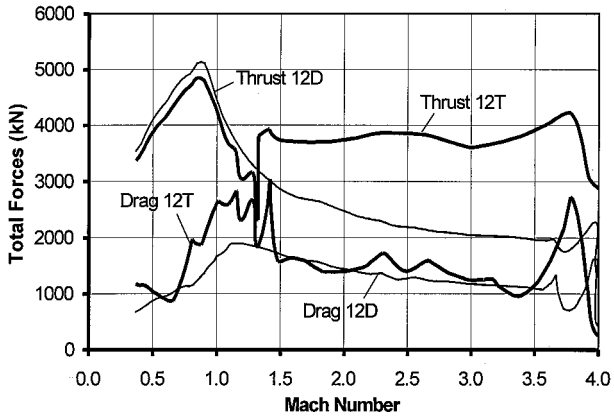

Fig. 14 Comparison of FSSC-12 ascent acceleration forces.

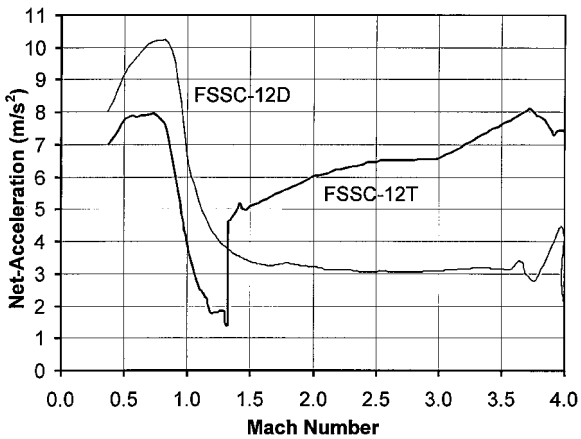

Fig. 15 Comparison of FSSC-12 net axial accelerations.

level of 105% nominal thrust is required. The typical thrust decrease of the turbojet engines is visible at higher Mach/altitude combinations where thrust enhancement is required by means of fuel rich combustion (EQR = 2.5) prior to the pull-up maneuver. Time to stage separation is 526 s, and the distance from Kourou is 378 km. The stage separation conditions are Mach 4.0, 25 km altitude, 3-deg flight-path angle. These results are a consequence of the weak net-acceleration potential of the turbojet engines at higher altitudes. Obviously this deficit cannot even be compensated with a refined aerodynamic design.

Despite the shortcomings in aerodynamic performance, the trapezoidal-wing configuration has completely fulfilled the FESTIP mission requirements and has remarkably exceeded the due cargo mass requirements (see Table 4, cargo = kick-stage plus spacecraft[8]). This is because the operation of the orbiter rocket engines in parallel to the turbojet engines of the first stage compensates for the characteristic aerodynamic losses and the inherent weakness

Table 4 Summary of FSSC-12 cargo mass capability into differently inclined 250-km reference orbits

Orbital inclination	98 deg	5 deg
Orbiter of FSSC-12 T ($m_{dry} = 31.39$ Mg; $m_p = 154.50$ Mg)		
Total takeoff mass, Mg	466.88	473.35
Stage separation Mach number	4.0	4.0
Stage separation altitude, km	30.3	30.3
Distance at stage separation, km	227.7	227.0
Orbiter liftoff mass, Mg	192.93	199.36
Cargo mass, Mg	2.99	9.00
Orbiter of FSSC-12 D ($m_{dry} = 31.24$ Mg; $m_p = 154.50$ Mg)		
Total takeoff mass, Mg	427.44	430.16
Stage separation Mach number	4.0	4.0
Stage separation altitude, km	26.0	24.9
Distance at stage separation, km	429.2	377.8
Orbiter liftoff mass, Mg	190.87	197.12
Cargo mass, Mg	1.21	7.07

of the turbojet engines at high Mach-number/altitude combinations. Because of the improvement of the aerodynamic performance of the delta-wing configuration in the end of the second design loop, and because of the increased thrust level of the turbojet engines (105% nominal thrust) and the increased equivalence ratio at Mach numbers beyond 3.5 the equatorial mission was fulfilled. But the cargo mass requirement of the polar mission was not met (Table 4). In principle the vehicle could be scaled up for improving polar mission performance. However, this would further increase development and operational cost. Further performance optimization of the delta-wing configuration is limited.

For designing a simple structure and maintaining an aircraft-like operation a hot structure concept was chosen for both vehicle options. In this context the slender body design and the fully integrated orbiter wing of the delta-wing configuration has involved severe structural penalties. The main reason is the unfavorable load beaming in both the delta-wing and the slender fuselage design. The nose gear does not directly support the forward stage-interface point, and the deep wing caving of the first stage requires an unconventional wing construction. As a result, the area masses are significantly higher than for the trapezoidal-wing configuration: 41.5 kg/m^2 (fuselage) and 58.1 kg/m^2 (wing) compared to 32.9 kg/m^2 and 40.3 kg/m^2, respectively. Another penalty is the positioning of the large vertical stabilizers at the wing trailing-edge area just above the nacelle integration. This was not included in the structural calculations. Area masses could be decreased only when applying more advanced materials and a protected structure with TPS (cold structure concept as for the orbiter), but resulting in an increased vehicle complexity. When implementing temperature-resistant composite materials like Fiberite, bismale-imide, and polyether-etherketone, significant mass savings can be expected.[9] The high structure masses of the two design options are mainly the reason for the high first-stage dry masses.

Based on the estimated mass budgets (Table 2), vehicle development cost was assessed with the PRICE-H cost calculation model. Both design options include the same baseline technology (materials, structural concept, engine concept). However, the development cost for the delta-wing first stage is higher by 17%. This can be explained by the following: 1) the first-stage dry mass is larger by 40 Mg (+27%); 2) the turbojet engines are larger by 2.1 Mg (+5%); 3) the delta-wing manufacturing is significantly more complex; and 4) the internal load transfer members of the fuselage are more complex; if compared to the trapezoidal-wing first stage.

A summary of these issues is given in Table 3. Uncertainty remains in both design approaches. Major unknowns are related to specific aerodynamic characteristics. The aerodynamic interaction effects that are expected between the wings of the trapezoidal-wing configuration could not sufficiently be explored because the support by computational fluid dynamics (CFD) calculations was only marginal. First wind-tunnel tests have been performed with a simplified small model at Technical University Aachen. Only for small wing-to-wing root distances critical flow conditions were found that

have led to local flow blockage. To further mitigate local interaction effects, a backward shift of the orbiter relative to the first stage may be helpful for avoiding shock-shock interactions.

In particular for the delta-wing configuration the aeorodynamic near-field effects during stage separation could not be assessed. From earlier SÄNGER investigations[10] it is known that such effects might affect the balance of forces and moments that have to be adjusted before with the combined configuration. Another open issue is the aerodynamic behavior of the caved vehicle upper side during fly-back.

Provided the aerodynamic uncertainties in the design of the trapezoidal-wing configuration can be solved, this concept is superior in all respects except aerodynamic performance. Orbiter engine operation in parallel to the airbreathing engines of the first stage is obviously a very effective mean for a pure acceleration ascent of the combined configuration. The high aerodynamic quality of the delta-wing configuration does not pay off for the current mission requirements. It may be favorable for missions with cruise segments such as the blended-body delta wing design of SÄNGER.

Conclusions

The FESTIP mission and system requirements have led to a new airbreathing TSTO launcher configuration with eight turbojet engines in the first stage and three rocket engines in the orbiter. The pure acceleration ascent has driven the first-stage design for maximum thrust minus drag, thus resulting in a wing-on-fuselage design. For the selected turbojet propulsion system of the first stage, the optimum stage separation Mach number is 4. Another airbreathing propulsion system (for example air-turbo-rocket or air-ejector-rocket) would drive up the optimium staging Mach number. Stage separation at Mach 4 has led to a large Orbiter with 193 Mg liftoff mass (polar mission). For covering opposite design ideas two different configurations of the first stage have been studied: the fully and the less integrated configuration options. The orbiter design was kept constant with respect to the limited manpower and time available for this launcher concept. A cold structure with TPS was assumed for the orbiter and a hot structure without TPS for the first stage.

The fully integrated TSTO option (delta-wing configuration) was designed to optimum aerodynamic performance with a slender body length of 86 m. Its takeoff mass is 430 Mg. It needs turbojet engines at 105% nominal size/thrust. The additional use of the orbiter rocket engines for thrust enhancement is not possible because of the high-stage integration level. The rocket engine plumes would impact the rear structure of the first stage, and the installation of additional tanks in the first stage would further worsen the volumetric situation in the slender fuselage. Stage integration and separation are most complex for this concept. A redesign of the cambered bottom of the orbiter could mitigate at least the geometric problems discovered.

The less integrated design option (trapezoidal-wing configuration) was designed to a simple and aircraft-like structure. Its takeoff mass is 473 Mg with a body length of 72 m. It needs the parallel operation of the orbiter rocket engines from Mach 1.3 up to Mach 4 to deliver the thrust that is required in addition to the turbojet engine thrust. In principle, the cross-feeding system slightly increases system complexity, but it was already successfully demonstrated in more than 94 space shuttle flights.

For both design options, the major deficiency is the aerodynamic database because CFD calculations and wind-tunnel testing were limited.

At the end of this FESTIP study, it can be concluded that for the present turbojet propulsion system and stage separation at Mach 4, the trapezoidal-wing option compared to the delta-wing option 1) provides better vehicle overall performance (3 Mg into polar and 9 Mg into equatorial reference orbit), 2) is less complex in the structural design and stage separation system, 3) has a high design flexibility with respect to changed requirements, and 4) promises 17% less development cost of the first stage because of the conventional manufacture of the structure and smaller turbojet engines.

A configuration of this type with stages that are mated belly to back would result in significant manufacturing and operations cost reductions.

References

[1]Kuczera, H., Sacher, P., and Dujarric, C., "FESTIP System Activities—Overview and Status," International Astronautical Federation, Paper 98-V.3.04, Sept.–Oct. 1998.

[2]Kuczera, H., and Hauck, H., "The German Hypersonics Technology Programme—Status Report 1992," International Astronautical Federation, Paper 92-0867, Aug. 1992.

[3]Grallert, H., and Berry, W., "Progress in ESA Winged Launcher Configurations Studies," International Astronautical Federation, Paper 91-199, Oct. 1991.

[4]Buhl, W., Ebert, K., and Herbst, H., "Optimal Ascent Trajectories for Advanced Launch Vehicles," AIAA Paper 92-5008, Dec. 1992.

[5]Grallert, H., and Herrmann, O., "Generic Derivation of a Promising Air-breathing TSTO Space Transportation System—From SÄNGER to FESTIP," AIAA Paper 98-1552, April 1998.

[6]Jenkins, D. R., Space Shuttle—The History of Developing the National Space Transportation System, Motorbooks International, Osceola, Wisconsin, 1993, p. 245.

[7]Rallu, P., Goncharov, N., and Haeseler, D., "RECORD Project Status (Russia-Europe Cooperation on Rocket Engine Demonstrator)," *Proceedings of the 5ième Symposium International sur la Propulsion dans les Transports Spatiaux, Association Aéronautique et Astronautique de France*, Paper 8.2, CNES and ESA, Paris, May 1996.

[8]Grallert, H., and Kuczera, H., "Kick-Stage—A Mandatory Element of Future Reusable Space Transportation Systems," AIAA Paper 99-4885, Nov. 1999.

[9]Brown, A. S., "Raptor Gives Composites a Lift," *Aerospace America*, No. 9/98, Sept. 1998.

[10]Kuczera, H., Krammer, P., and Sacher, P., "SÄNGER and the German Hypersonics Technology Programme—Status Report 1991," International Astronautical Federation, Paper 91-198, Oct. 1991.